Dynamical Behavior Of Disk Type Closed Cycle MHD Generator

Author(s): Y. Yoshikawa, S. Kabashima, H. Yamasaki, N. Harada, and S. Shioda

Session Name: Disk Generators

SEAM: 22 (1984)

SEAM EDX URL: https://edx.netl.doe.gov/dataset/seam-22

EDX Paper ID: 1048

DYNAMICAL BEHAVIOR OF DISK TYPE CLOSED CYCLE MHD GENERATOR

Y.Yoshikawa, S.Kabashima, H.Yamasaki, N.Harada, and S.Shioda
Tokyo Institute of Technology, Nagatsuta,Midori-ku,
Yokohama 227, Japan

ABSTRACT

Behavior of closed cycle MHD plasma in a disk generator is studied by solving time-dependent MHD equations. The fully ionized seed state is obtained as the final state for several conditions of working gas. The relaxation region near the inlet of the channel is examined for some different inlet conditions.

INTRODUCTION

It is shown theoretically and experimentally that the power reduction due to the ionization instability in the closed cycle MHD power generation can be eliminated by the concept of the fully ionized seed.(1) The experiments and steady state analyses performed by the group of Tokyo Institute of Technology have shown the advantage of the disk type generator with fully ionized seed.(2-7)

It is, therefore, important to confirm the dynamical realization of the fully ionized seed state in the MHD channel.

In the 21st symposium we have shown some result of the dynamical properties of the closed cycle MHD plasma in a disk type channel.(8) Here we will report more extended results of the numerical analysis regarding this problem. The realization of the fully ionized state is obtained for working gas helium as well as that for working gas argon. The relaxation region near the inlet of the disk becomes narrower in the case of wroking gas helium as compared with argon.

BASIC EQUATIONS AND PROCEDURE OF CALCULATION

The calculation is based on the two temperature model equations of the closed cycle MHD power generation(9-12) and an assumption of the weak interaction generator. In the two temperature model the equations of MHD plasma are shown as:

$$\frac{\partial n_e}{\partial t} + \nabla\cdot(n_e \vec{u}_e) = \dot{n}_e \,, \tag{1}$$

$$\vec{j} + \frac{\beta}{B}\vec{j}\times\vec{B} = \sigma\vec{E} + \frac{k}{en_e}\nabla P_e \,, \tag{2}$$

$$\frac{\partial U_e}{\partial t} + \nabla\cdot(U_e \vec{u}_e) = \frac{j^2}{\sigma} - A - \nabla\cdot(p_e \vec{u}_e) - \nabla\cdot\vec{q}_e - Q_r \,, \tag{3}$$

where

$$\dot{n}_e = k_f n_e n_A - k_r n_e^3 \,,$$

$U_e = (3/2)n_e kT + \varepsilon_N n_N^+ + \varepsilon_S n_S^+$,

A : energy loss of due to collisions ,

$\nabla \cdot \vec{q}_e$: thermal conductive energy loss ,

Q_r : radiative energy loss ,

and other notations used are same as given in the papers referred in 6 to 12 .

The channel size is determined by considering the characteristic length of the plasma and it is shown in Table 1, where the equal cross section of channel is assumed. The conditions of the working gas and magnetic fields listed in Table 2 are selected to get the stable plasma from quasi one dimensional calculation.(7) As an inlet boundary condition an electron temperature of 3500K is adopted to simplify the calculation but it is not so far from real condition. Because the plasma radiation can be observed even in a nozzle in shock tunnel experiments in T.I.T. The inlet conditions of electron density for calculations are shown in Table 2 and the other procedures and assumptions are same as given in the 21st symposium.

RESULTS AND DISCUSSIONS

The evolution of average electron temperature T_e and electron number density n_e over the channel are shown in Fig 1 (a), where the average value is defined as:

$$T_e = \frac{\sum_{i=1}^{N} n(i)T(i)}{\sum_{i=1}^{N} n(i)} \quad (4) \quad , \quad n_e = \frac{\sum_{i=1}^{N} n(i)}{N} \quad , \quad (5)$$

$n_e(i)$ and $T_e(i)$ represents the electron number density and electron temperature at the i'th mesh element, and N is total number of the elements. This figure shows that approximately at 5 μsec the T_e and n_e reaches the steady value. Fig.1(b) shows distributions of potential (ϕ),electron temperature (T_e) and current stream function (ψ) inside the whole channel,where ϕ and ψ are introduced using the channel height h as :

$$E_r = -\frac{\partial \phi}{\partial r} \quad , \quad E = -\frac{1}{r}\frac{\partial \phi}{\partial \theta} \quad , \quad (6)$$

$$j_r = \frac{1}{rh}\frac{\partial \psi}{\partial \theta} \quad , \quad j_\theta = -\frac{1}{h}\frac{\partial \psi}{\partial r} \quad . \tag{7}$$

This figure shows that distribution of T_e is highly disturbed approximately at 4 μsec and as the time increase the disturbance becomes weak except near the inlet region.

At the end point of the time interval of the numerical calculation, the disturbance in the electron temperature (T_e) exists at the inlet region of the channel where T_e increases from 3500K to a higher value, and this region is called as the relaxation region. At this region the electrical conductivity is low as a result of the direction of current stream becomes opposite to that of uniform region. In the uniform region the fully ionized seed is achieved. (i.e. the rate of ionization of potassium is unit)

Figs.2(a) and (b) show the results obtained from the numerical calculation using argon seeded with potassium as working gas and taking the inlet electron number density as one-third of the Saha electron number density. The effect of changing the electron number density from 1/2 to 1/3 of Saha value in the numerical calculation did not show any prominent change in the variation of average electron temperature and average electron number density with time and also the change in the distribution of potential , electron temperature and current stream function was not found much. The results also show that at the end point of time interval of numerical calculation, the relaxation region near the inlet of the channel did not change with the change of the electron number density from 1/2 to 1/3 of the Saha value. Later we will discuss about the change of the area of the relaxation region in details, where the electron temperature distribution in radial direction will be discussed.

When argon seeded with Cs is used as the working gas the average electron temperature and the average electron density reach steady region faster as shown in Fig.3 (a), where other conditions are similar to those in Fig 1. The uniformity of the electron temperature distribution also reaches steady region faster in the case of Cs-seeded argon gas as compared with K-seeded argon gas. These results are expected from the fact that the ionization potential of cesium is lower than that of potassium.

Using He as inert gas in place of argon and keeping Mach number inside the channel the same as in case of argon, we obtain the results shown in Fig.4(a) and (b),where potassium is used as the seed material. Since the gas velocity in this case is about three times higher than that of argon, the results obtained from the numerical calculation show that the tangential current density becomes higher as a result joul heating also becomes higher. However the wider relaxation region compared to that of Ar is observed from the high velocity of gas, even though joul heating is higher in the case of He. The results show that the average electron temperature and electron number density nearly reach the steady value, and the load resistance lies in the stable region of the V-I curve of fully ionized seed condition. But in this case the relaxation region at the channel inlet is wider as a result the effective conductivity σ_{eff} and Hall parameter β_{eff} inside the whole channel become half of the ideal value.

Figs.5 (a) and (b) show the results when the seed material is changed from K to Cs. Seeded Cs lies almost in the ionized state even in the initial state of calculation due to the low ionization potential. Fig.5(b) shows that at the end point of the time interval of numerical calculation

the relaxation region is as wide as in the case of potassium seeded argon gas and occupy nearly half of the channel area and the effective value of the conductivity and Hall parameter become half of the ideal value.

In Fig.6 electron temperature averaged over tangential direction is plotted along the radial direction for the conditions shown in Figs 1 to 5. The length from the inlet to the point indicated by arrow is interpreted as relaxation length.(ref.8) From Fig.6(a) and (b) which show the result obtained from the numerical analysis using argon seeded with potassium as working gas it is found that the electron distribution inside the channel and the relaxation region are almost same in both case (a) and (b) even where the electron number densities are taken as 1/2 and 1/3 of Saha equilibrium value, respectively. We can see from these figures that the relaxation length is not so much affected by the difference of the inlet electron number density, but the minor difference of the tangential distribution of electron temperature and electron number density can be observed. It is found from the electron temperature distributions along the radial direction that the fully ionized seed plasma is obtained at about 3cm from the inlet for both the condition of inlet electron number densities of 1/2 and 1/3 Saha equilibrium value, respectively.

The results obtained from the numerical calculation using argon seeded with cesium as working gas and taking the inlet n_e = 1/2 Saha value are shown in Fig 6 (c). Comparison of Fig 6(c) with Fig 6 (a) show that the relaxation length for Cs seeded plasma is shorter than that for K seeded plasma. From this comparison we can infer that the uniformity of electron temperature distribution inside the whole channel is better for Cs as a seed material.

Fig 6(d) shows the radial electron temperature distribution obtained under the condition that the working gas is helium seeded with potassium and the inlet n_e = 1/2 Saha equilibrium value. For the present condition of numerical calculation it is found that the relaxation length covers about 40% of the whole channel radius. This effect can be explained by the fact that the helium gas velocity is about three times higher than that of argon gas as a result the relaxation region in the case of He + K much blow away as compared with the case of Ar + K.

Fig 6 (e) shows the radial electron temperature distribution obtained under the condition that the working gas is helium seeded with cesium and the inlet n_e = 1/2 Saha equilibrium value. Comparison of the present case result with that of Fig 6 (d) show that even if the seed fraction in the present case was half of that of Fig 6 (d) case but the relaxation region did not differ much in these two cases, though the low seed fraction and low ionization potential should produce narrow relaxation region. It is found from comparison between the results of numerical calculation using argon seeded with potassium and argon seeded with cesium as the working gas and taking all other condition similar in both cases that the relaxation length differ very much in those two cases. But in the case of helium change of seed material from potassium to cesium did not affect the relaxation length much, which can be explained by the fact that the effect of velocity . plays a dominant role rather than the effect of ionization potential difference of the seed materials. In the case of helium as working gas, further analyses should be needed to get better condition of working gas.

CONCLUDING REMARKS

In the case of argon as back ground gas the stable region is dynamically achieved by the fully ionized seed and better uniformity is expected to obtain near the channel inlet and also not much change in

relaxation length is expected as a result of slight change in inlet condition. If proper matching of the gas condition and the load resistance is done then relaxation length is expected to become shorter.

In the case of helium as inert gas as compared with argon, if the seed material and seed fraction is changed, the relaxation length is not expected to change much which can be explained by the fact that the velocity in the case of inert gas helium is about three times faster than that of argon. To achieve better uniformity proper matching of the gas condition and the load resistance will be carried out numerically later on by the authors.

It is a great pleasure for the authors to thank Mr. D.Biswas for his helpful disccussion.

REFERENCES

1. T.Nakamura and W.Riedmüller, "Stability of Noneuilibrium MHD Plasma in the Regime of Fully Ionized Seed", AIAA Joural 12 661 (1974)
2. S.Shioda and H.Yamasaki, "Experimental Studies of Linear MHD Generator with Fully Ionized Seed", Journal of Energy 2 337 (1978)
3. S.Shioda, H.Yamasaki, K.Matsutani and H.Sato, "Experimental Studies on an Inert Gas Disk Generator with a Small Seed Fraction", Proc. 18th Symp. Engng. Aspects MHD, d.2.6.1 (1979)
4. S.Shioda, H.Yamasaki, T.Abe, R.P.Dahiya, S.Saito and Y.Shimazu, "Power Generator Experiments and Prospect of Closed Cycle MHD with Fully Ionized Seed", Proc. 7th Int. Conf. MHD, Vol II, 685 (1980)
5. H.Yamasaki, N.Harada, R.P.Dahiya, S.Saito, K.Yoshikawa, S.Kabashima and S.Shioda, "Effect of Inpurities and Gas Temperature on Closed Cycle MHD Generator with Fully Ionized Seed", Proc. 19th Symp. Engng Aspects MHD,7.4.1 (1981)
6. T.Abe, S.Kabashima, H.Yamasaki, and S.Shioda, "Theoretical Studies on Closed Cycle MHD Generator with Fully Ionized Seed", Proc. 19th Symp. Engng. Aspects MHD,7.5.1 (1981)
7. T.Abe, S.Kabashima, H.Yamasaki, and S.Shioda, "Numerical Studies of a High Interaction MHD Generator with Fully Ionized Seed", Engng. Convers. Mgmt. 22 251 (1982)
8. S.Kabashima, Y.Yoshikawa, H.Yamasaki, N.Harada and S.Shioda, "Dynamical Behavior of Disk Type Closed Cycle MHD Generator", Proc. 21st Symp. Engng. Aspects MHD,6.3.1 (1983)
9. R.J.Rosa, Magnetohydrodynamic Energy Conversion p.37 MacGraw-Hill New York (1963)
10. J.D.Tare, W.J.Loubsky, J.K.Lytle and J.F.Louis, "Opimization of Disk Generator Performance for Base-Load Plant Systems Aplication", 7th Int. Conf. MHD, Vol II,644 (1980)
11. P.Masse, "Performance of Closed Cycle Disk Generator Operating with Stable or Unstable Plasma", Proc. 19th Symp. Engng. Aspects MHD,7.1.1 (1981)
12. T.Hara, A.Veefkind, L.H.Th.Rietjens, "Numerical Simulation of the Inhomogeneous Discherge Structure in Noble Gas MHD Generators", AIAA Journal 20 1473 (1982)

Table 1. Disk size

Inlet radius	0.1 m
Outlet radius	0.2 m
Cross section	1.25×10^{-2} m^2

Table 2. Working gas conditions

Inert Gas	Seed	Stagnant Pressure (atm)	Stagnant Temperature (K)	Seed Fraction	Mach Number	Magnetic Field Strength (T)	Load Resistance (Ω)	Inlet Ne (xsaha equilibrium value)
Ar	K	6	2000	6.0×10^{-5}	1.7	3.5	0.78	1/2
Ar	K	6	2000	6.0×10^{-5}	1.7	3.5	0.78	1/3
Ar	Cs	6	2000	6.0×10^{-5}	1.7	3.5	0.78	1/2
He	K	4	2000	6.0×10^{-5}	1.7	7.0	1.15	1/2
He	Cs	4	2000	3.0×10^{-5}	1.7	7.0	2.05	1/2

SEAM #22 (1984), Session: Disk Generators

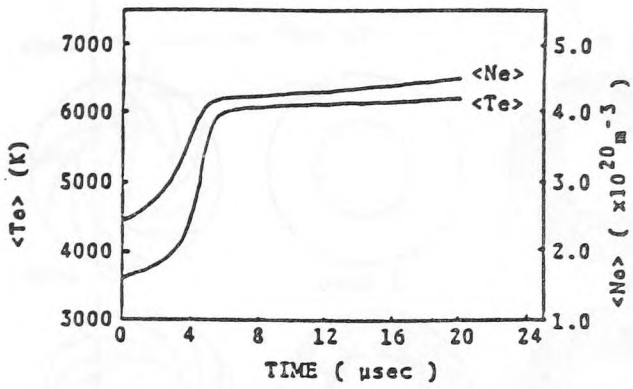

(a)

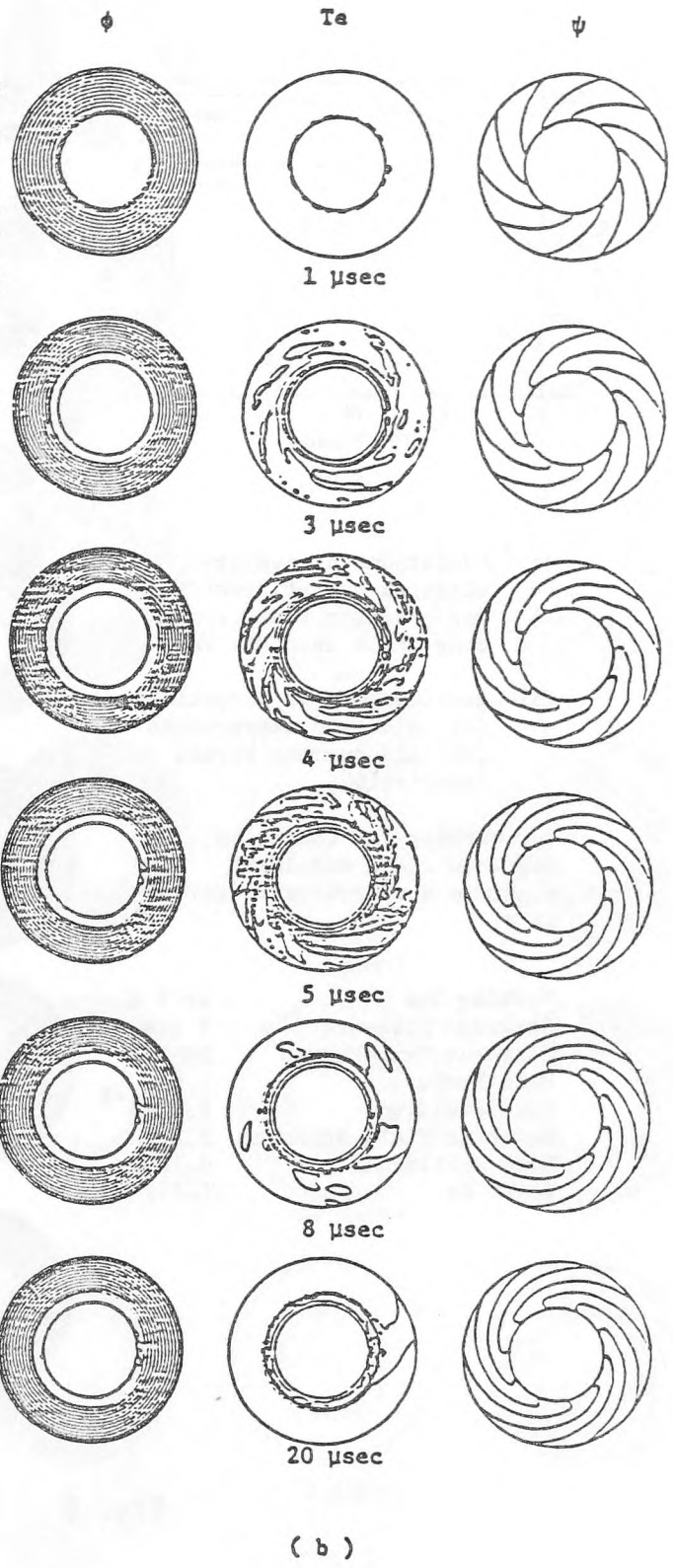

(a) Evolutions of average electron number density and electron temperature over whole channel, and

(b) developments of potential (ϕ), electron temperature (Te) and current stream fanction(ψ),

for working gas condition, magnetic field and inlet electron number density given as :

Working Gas	Ar + K
Stagnant Pressure	6 atm
Stagnant Temperature	2000 K
Mach Number	1.7
Seed Fraction	6.0×10^{-5}
Magnetic Field Strength	3.5 T
Load Resistance	0.78 Ω
Inlet Ne	(1/2) saha

Fig. 1

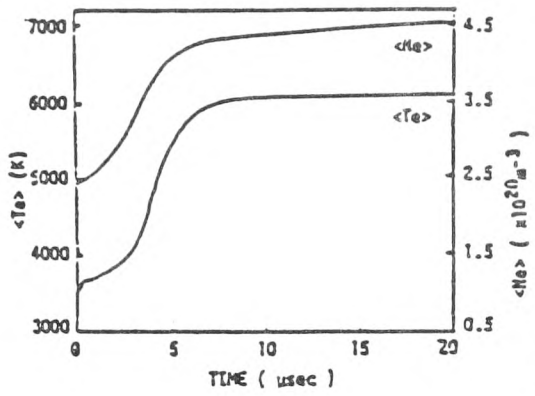

(a)

(a) Evolutions of average electron number density and electron temperature over whole channel, and

(b) developments of potential (ϕ), electron temperature (Te) and current stream function(ψ),

for working gas condition, magnetic field and inlet electron number density given as :

Working Gas	Ar + K
Stagnant Pressure	6 atm
Stagnant Temperature	2000 K
Mach Number	1.7
Seed Fraction	6.0×10^{-5}
Magnetic Field Strength	3.5 T
Load Resistance	0.78 Ω
Inlet Ne	(1/3) saha

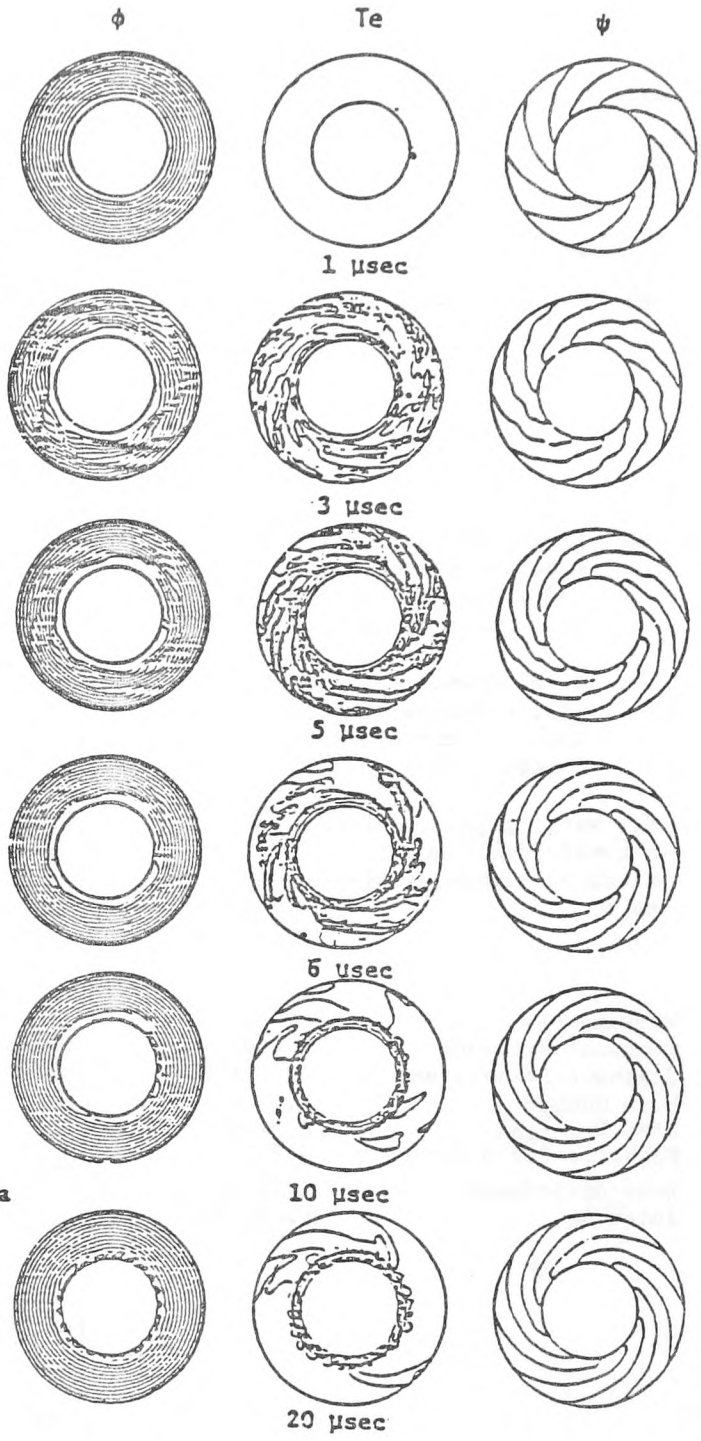

(b)

Fig. 2

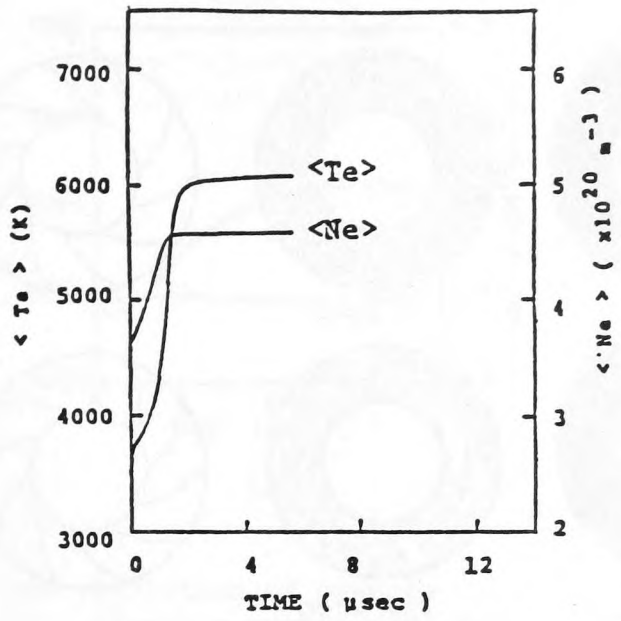

(a)

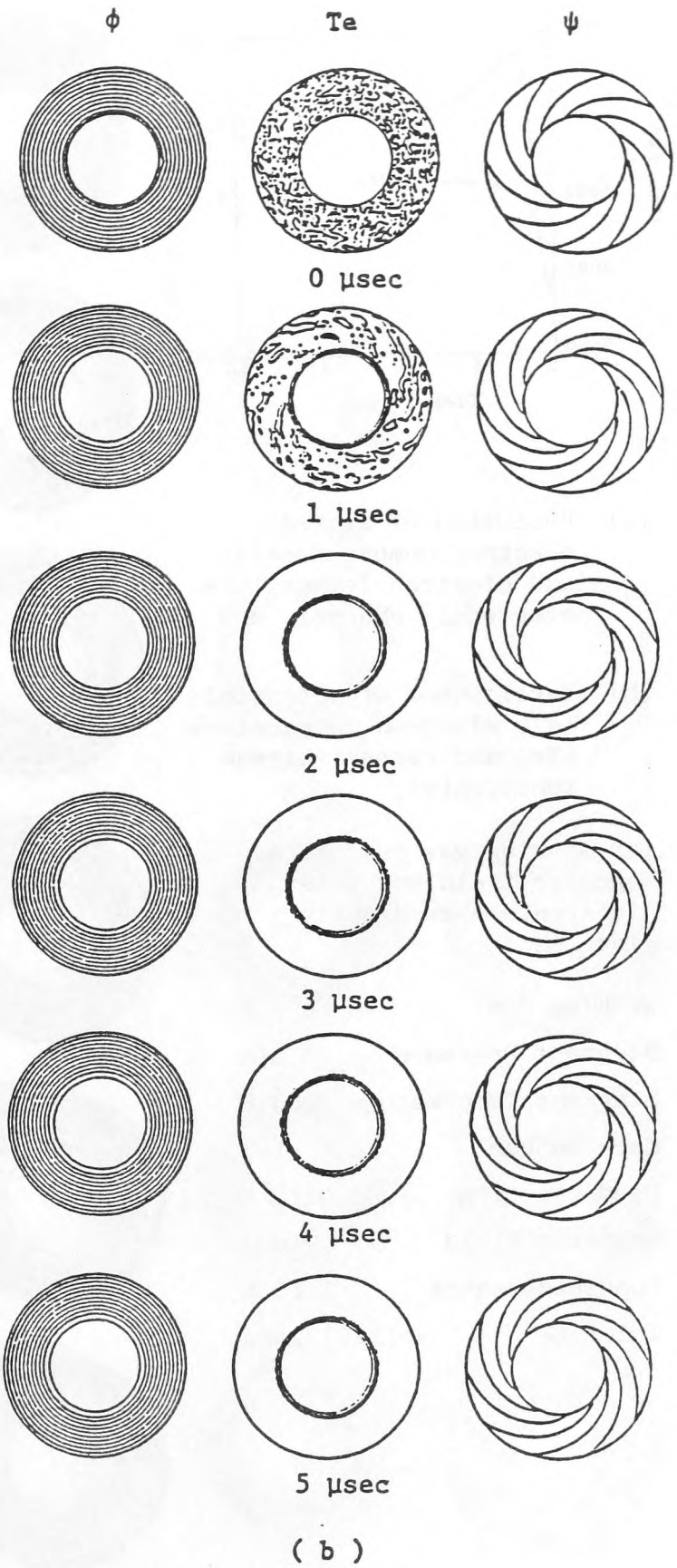

(b)

(a) Evolutions of average electron number density and electron temperature over whole channel, and

(b) developments of potential (ϕ), electron temperature (Te) and current stream fanction(ψ),

for working gas condition, magnetic field and inlet electron number density given as :

Working Gas	Ar + Cs
Stagnant Pressure	6 atm
Stagnant Tenperature	2000 K
Mach Number	1.7
Seed Fraction	6.0×10^{-5}
Magnetic Field Strength	3.5 T
Load Resistance	0.78 Ω
Inlet Ne	(1/2) saha

Fig. 3

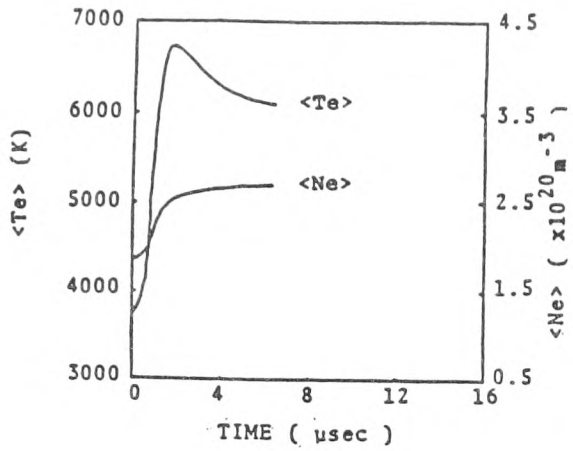

(a)

(a) Evolution of average electron number density and electron temperature over whole channel, and

(b) development of potential (ϕ), electron temperature (Te) and current stream function(ψ),

for working gas condition, magnetic field and inlet electron number density given as :

Working Gas	He + K
Stagnant Pressure	4 atm
Stagnant Temperature	2000 K
Mach Number	1.7
Seed Fraction	6.0×10^{-5}
Magnetic Field	7.0 T
Load Resistance	1.15 Ω
Inlet Ne	(1/2) saha

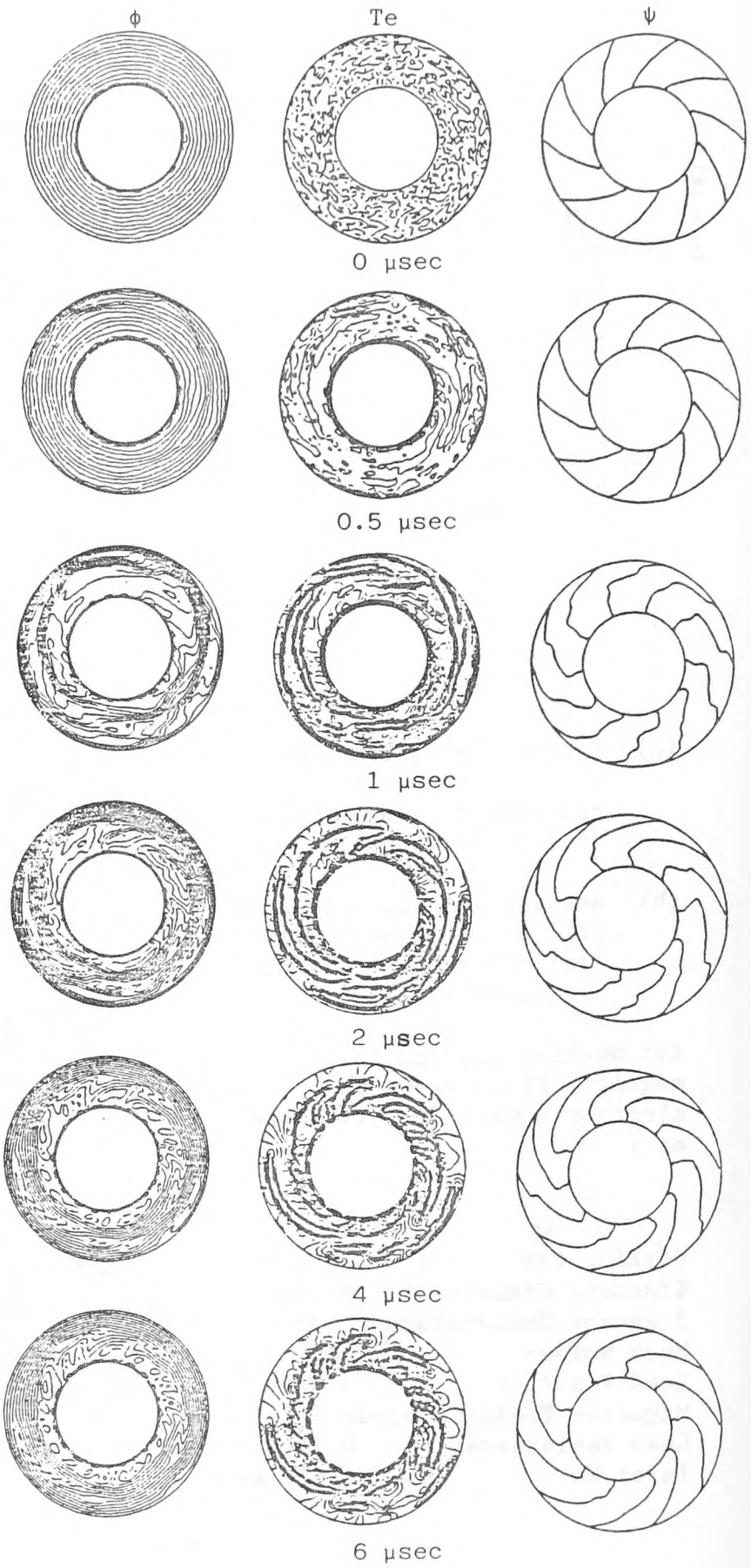

(b)

Fig. 4

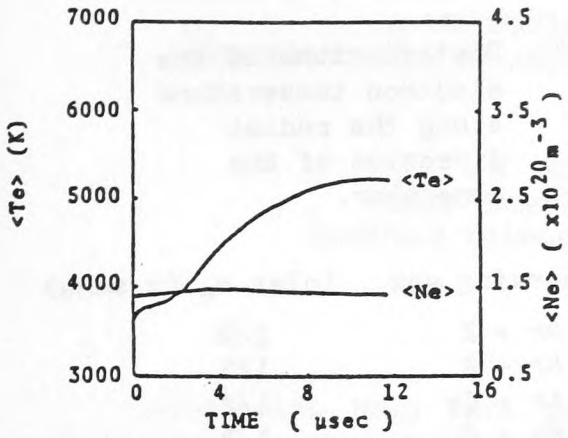

(a)

(a) Evolution of average electron number density and electron temperature over whole channel, and

(b) development of potential (ϕ), electron temperature (Te) and current stream function(ψ),

for working gas condition, magnetic field and inlet electron number density given as :

Working Gas	He + Cs
Stagnant Pressure	4 atm
Stagnant Temperature	2000 K
Mach Number	1.7
Seed Fraction	3.0×10^{-5}
Magnetic Field	7.0 T
Load Resistance	2.05 Ω
Inlet Ne	(1/2) saha

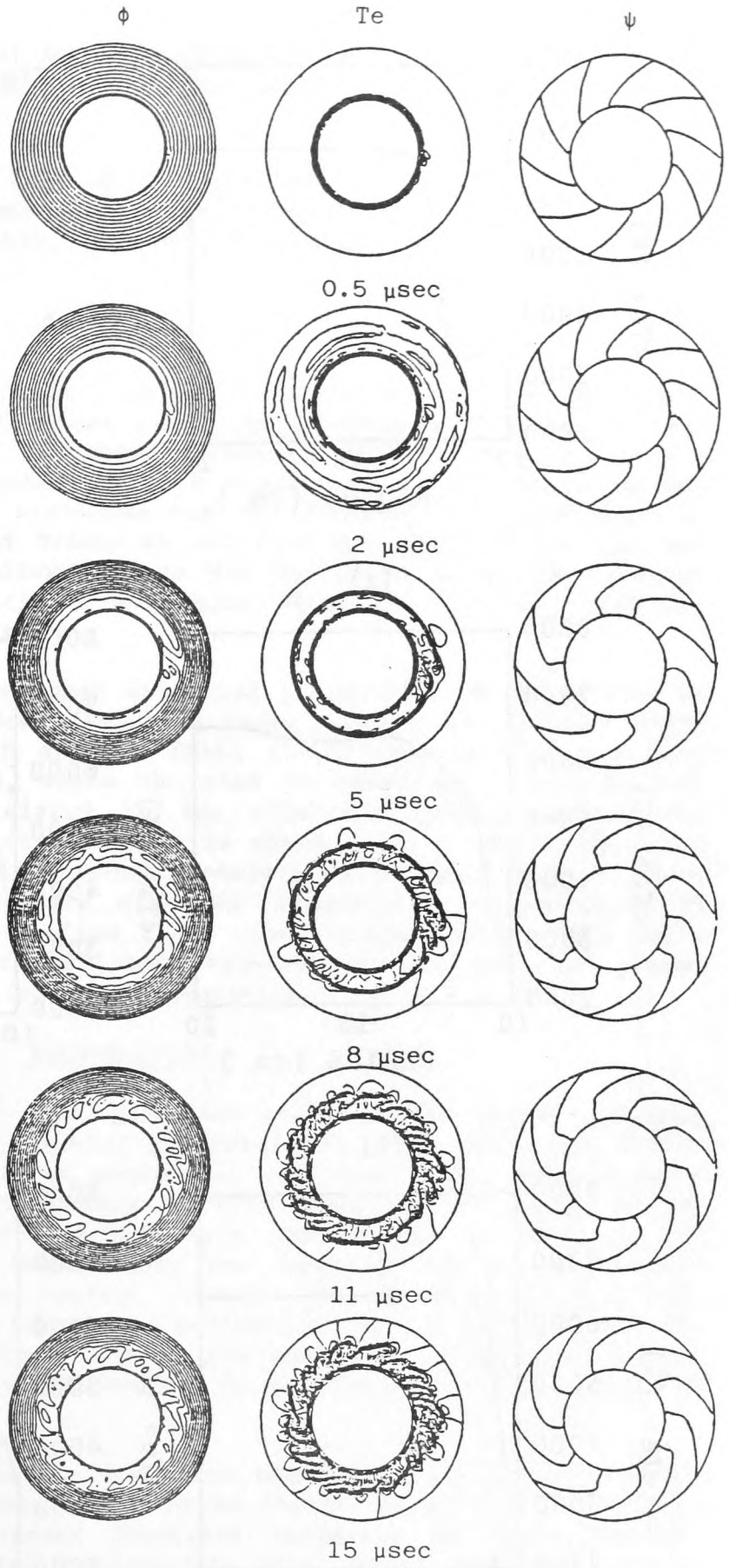

(b)

Fig. 5

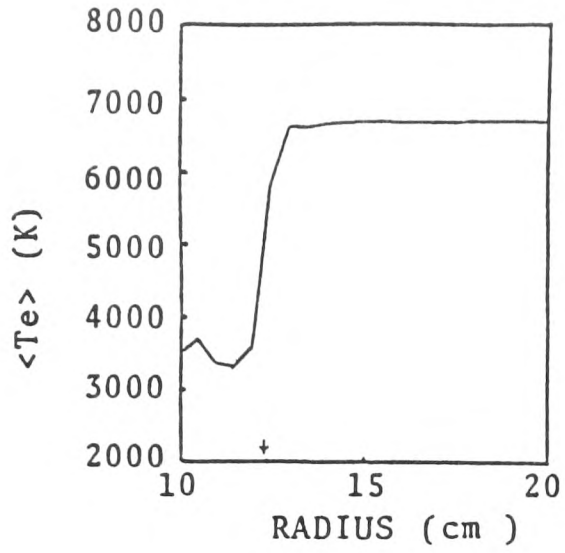

(a)

Fig.6 Distributions of the electron temperature along the radial direction of the generator.

	working gas	inlet n_e (x saha)
a	Ar + K	1/2
b	Ar + K	1/3
c	Ar + Cs	1/2
d	He + K	1/2
e	He + Cs	1/2

The other conditions are given in Table 2.

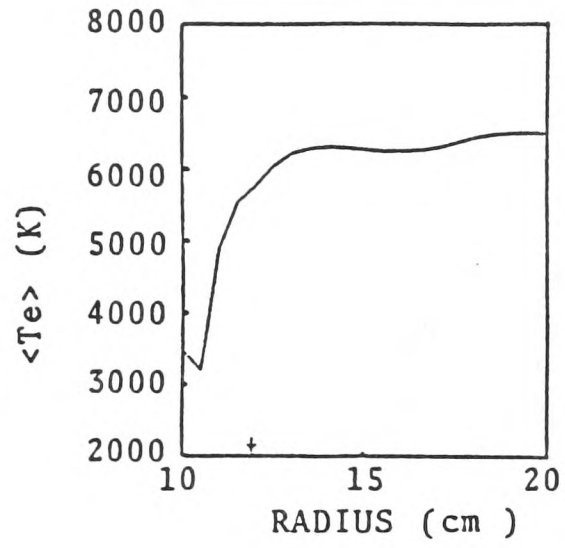

(b)

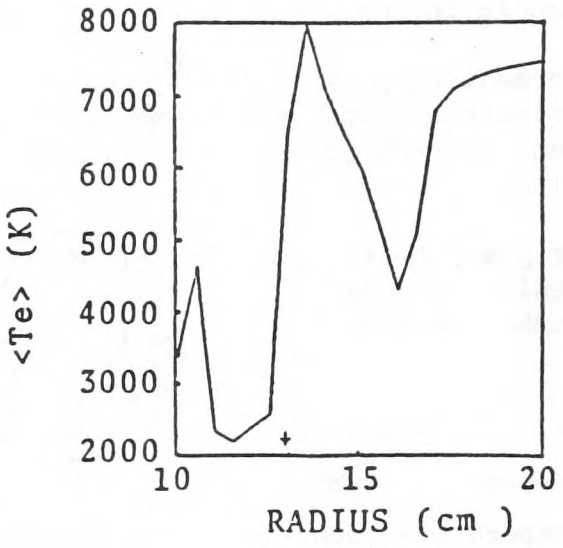

(d)

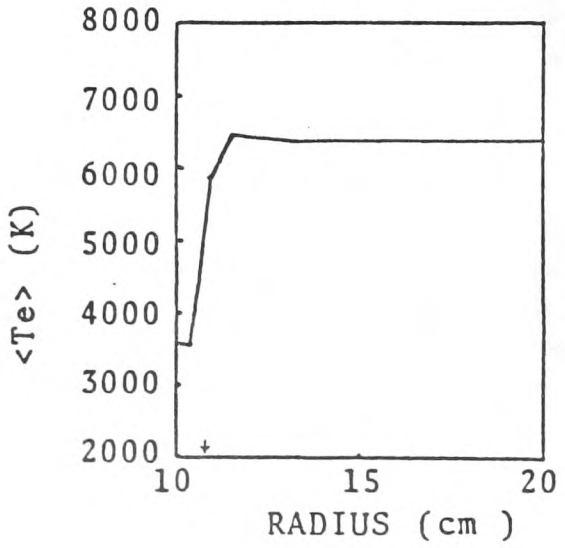

(c)

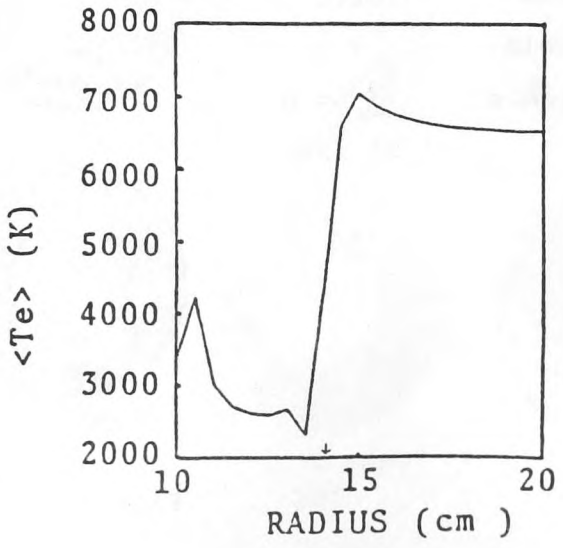

(e)